

Supplementary data

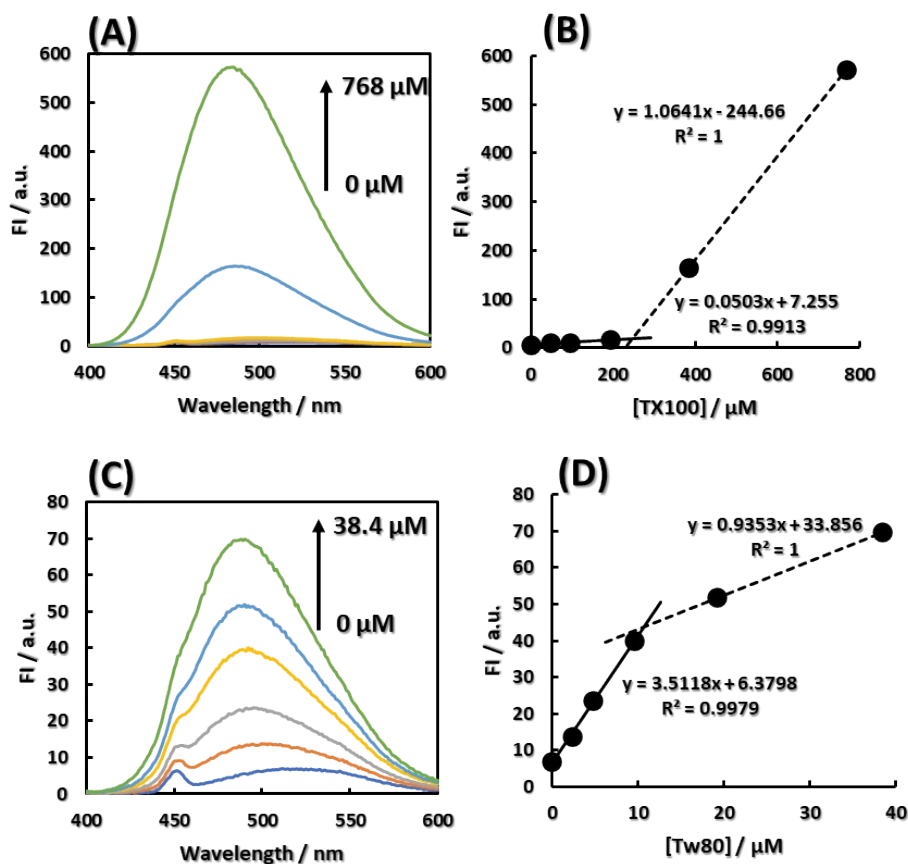


Figure. S1. Concentrations of TX100 and Tw80, which are 0.8 times the literature value of CMC, maximize its effectiveness as a monomer. (A): Fluorescence spectra of 0, 48, 96, 192, 384 and 768 μM TX100 in the presence of 10 μM ANS. (B): The vertical axis is the peak intensity of (A), and the horizontal axis is the TX100 concentration. (C): Fluorescence spectra of 0, 2.4, 4.8, 9.6, 19.2 and 38.4 μM Tw80 in the presence of 10 μM ANS. (D): The vertical axis is the peak intensity of (C), and the horizontal axis is the Tw80 concentration.

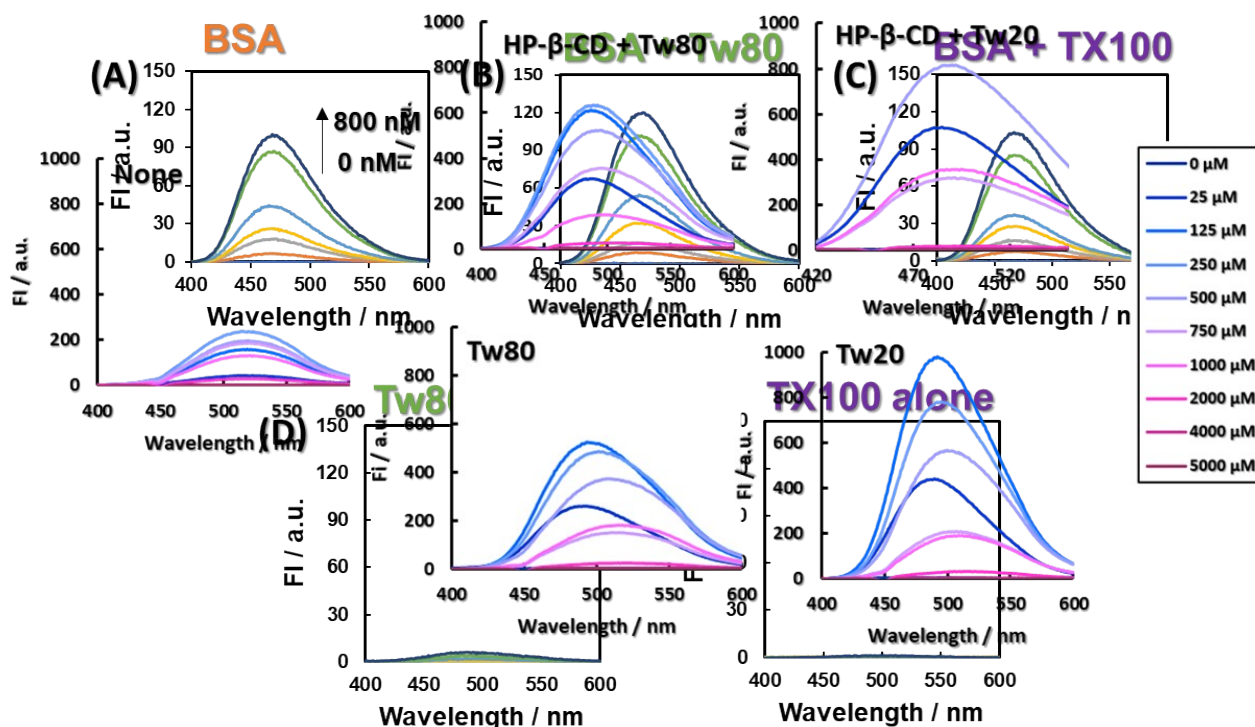


Figure. S2. Fluorescence caused by the binding of ANS to BSA. The upper three graphs show fluorescence spectra of 100 nM BSA in the presence of various concentrations of ANS with and without Tw80 or TX100. The lower two graphs show the fluorescence spectra of Tw80 or TX100 in the presence of various concentrations of ANS. [ANS] = 0, 20, 50, 100, 200, 500, 800 nM, [BSA] = 100 nM, [Tw80] = 9.6 μ M, [TX100] = 192 μ M.

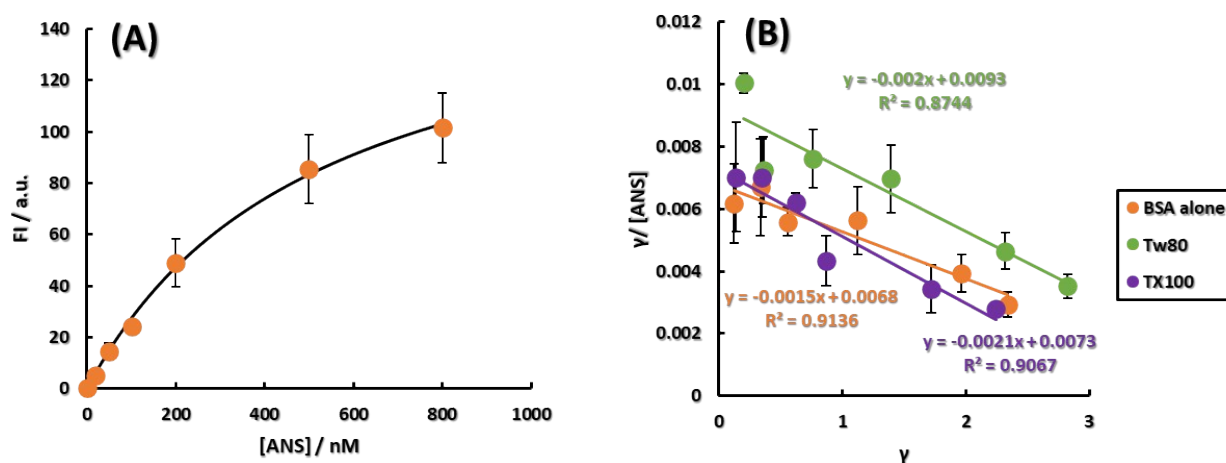


Figure. S3. Analysis of ANS adsorption to BSA. (A): The plots are ANS fluorescence intensity at various concentrations of ANS with 100 nM BSA. The curve is Eqn (1) fitted to the plots. (B): The Scatchard plot was applied to Fig. 1A.

Figure. S4. ANS concentration-dependent generation of quenched ANS molecules in the absence and presence of HP- β -CD, various non-ionic surfactants. [ANS] = 0, 25, 125, 250, 500, 750, 1000, 2000, 4000 and 5000 μ M.

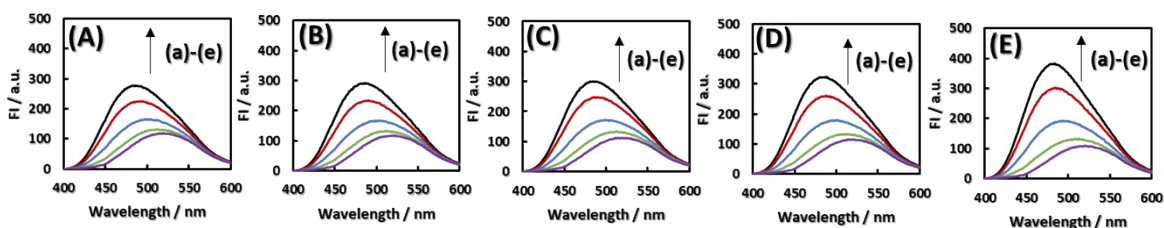


Figure. S5 HP- β -CD concentration-dependent blue shift and increase in fluorescence intensity of ANS fluorescence in the presence of various concentrations of NaCl. (A): 0 M NaCl; (B): 0.1 M NaCl; (C): 0.2 M NaCl; (D): 0.4 M NaCl; (E): 0.8 M NaCl. (a)-(e): 0, 2.5, 7.5, 15, 20 μ M HP- β -CD, respectively. [ANS] = 75 μ M.

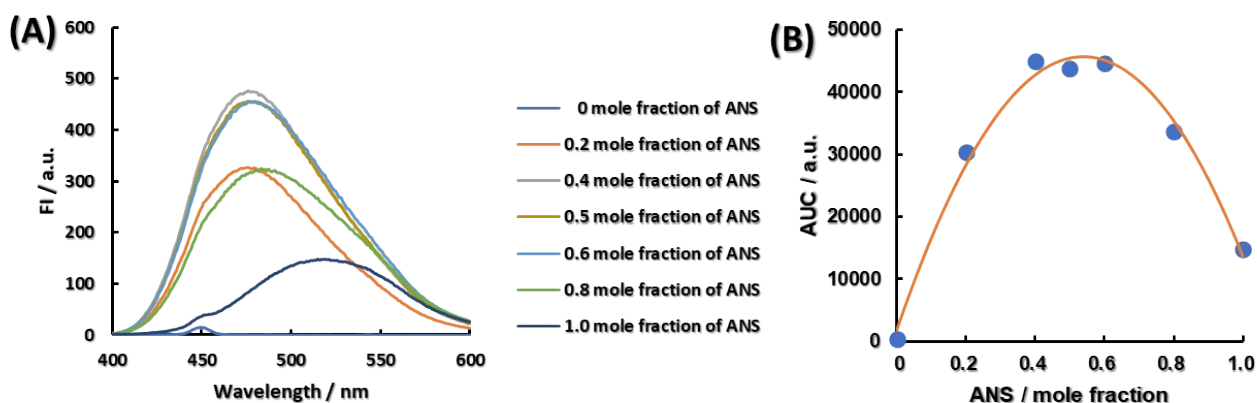


Figure. S6 Formation of 1:1 complex by HP- β -CD and ANS. The AUC of these fluorescence spectra (A) were used to generate Job's plot shown in (B). [ANS] + [HP- β -CD] = 100 μ M.

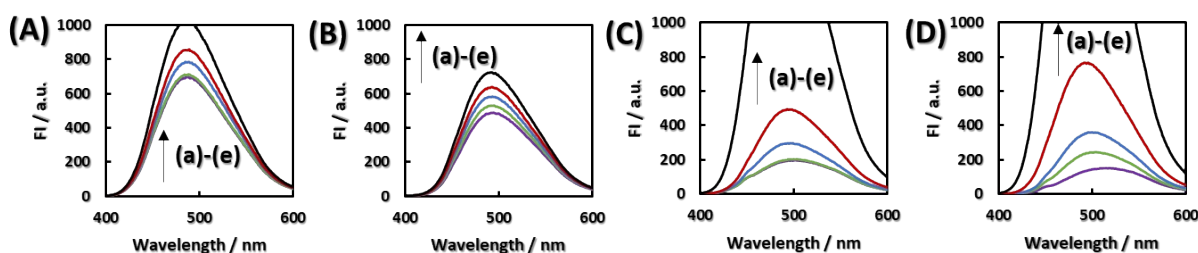


Figure. S7 Response of ANS Fluorescence to NaCl Concentration in the Presence of HP- β -CD, in the Presence of Surfactant, or in the Presence of Both. (A): in the presence of HP- β -CD and Tw80; (B): in the presence of Tw80; (C): in the presence of HP- β -CD and TX100; (D): in the presence of TX100. (a)-(e): 0, 0.1, 0.2, 0.4, 0.8 M NaCl, respectively. [ANS] = 75 μ M, [HP- β -CD] = 20 μ M.

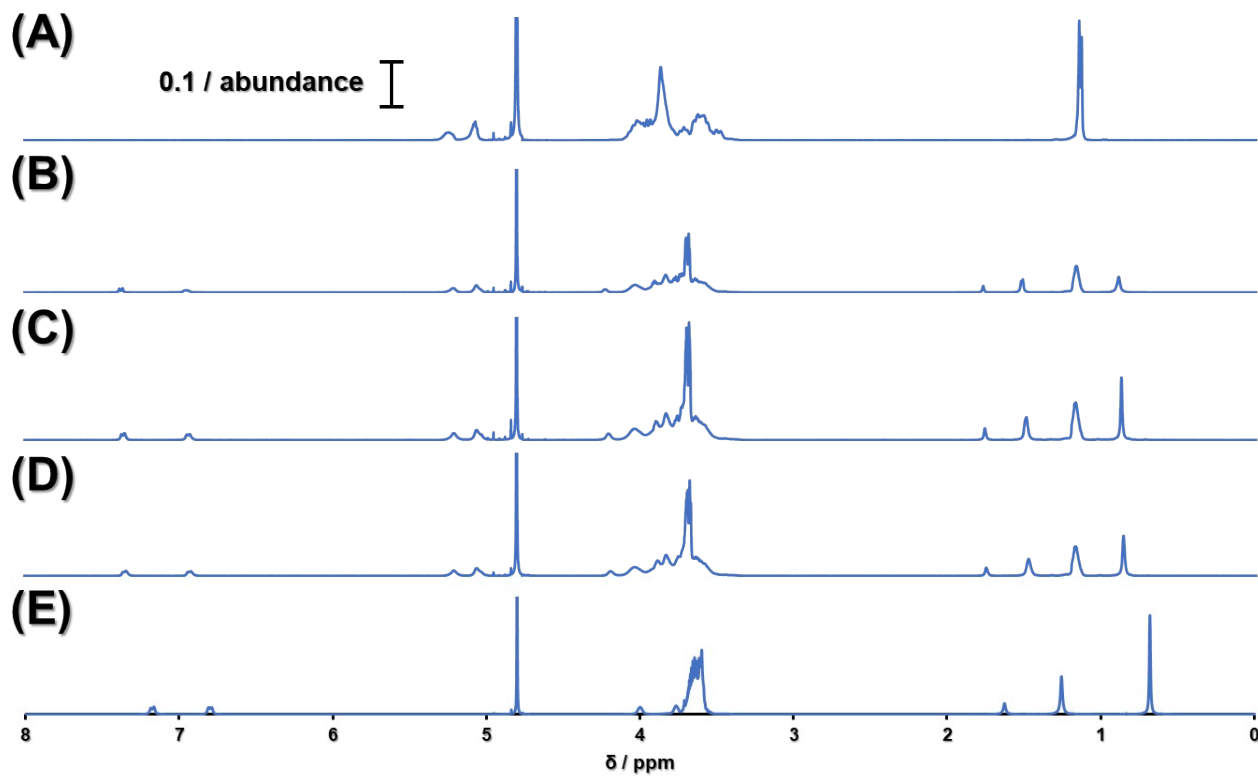


Figure. S8. HP- β -CD concentration-dependent low magnetic field shift in the protons of the alkyl chain and benzene ring of TX100. These are the $^1\text{H-NMR}$ spectra at various concentrations of HP- β -CD and TX100. (A); HP- β -CD, (B); 1:1, (C); 1:2, (D); 1:3, (E); TX100. The deuterium signal in D_2O (4.72 ppm) was used as an internal lock signal.

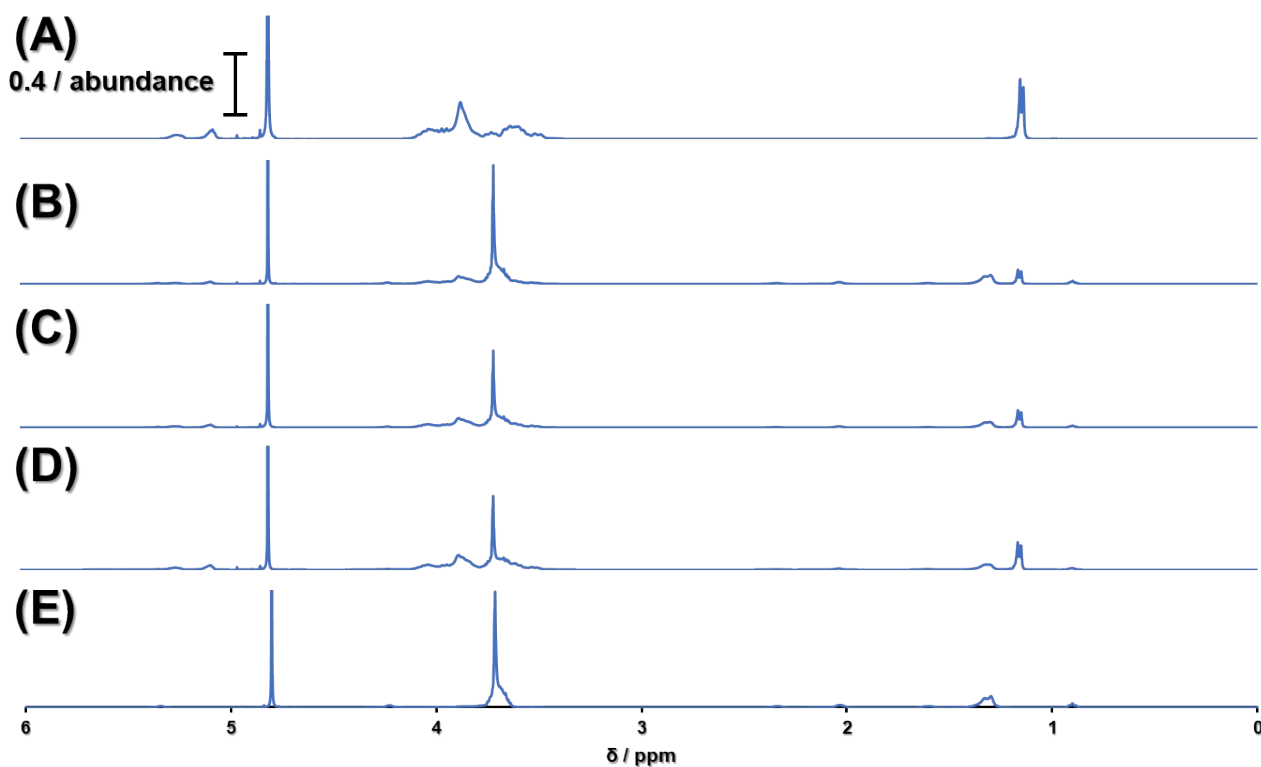


Figure. S9. The peak peculiar to Tw80 did not show an HP- β -CD concentration-dependent shift. These are the ^1H -NMR spectra at various concentrations of HP- β -CD and Tw80. (A); HP- β -CD, (B); 1:1, (C); 1:2, (D); 1:3, (E); Tw80. The deuterium signal in D_2O (4.72 ppm) was used as an internal lock signal.

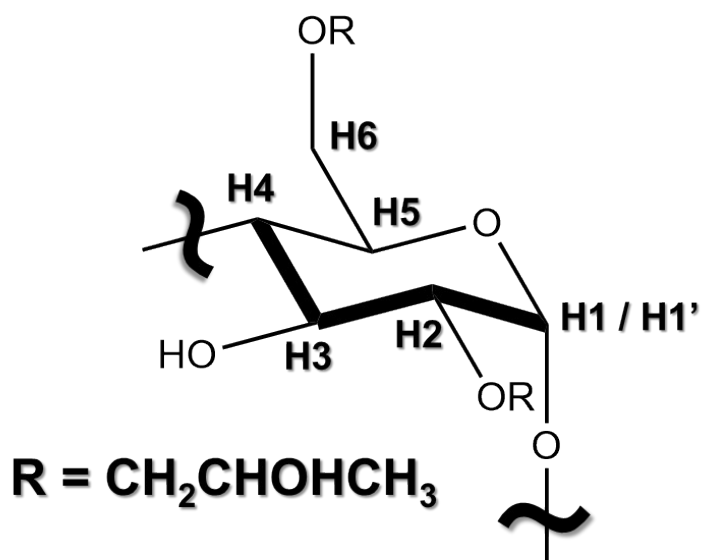
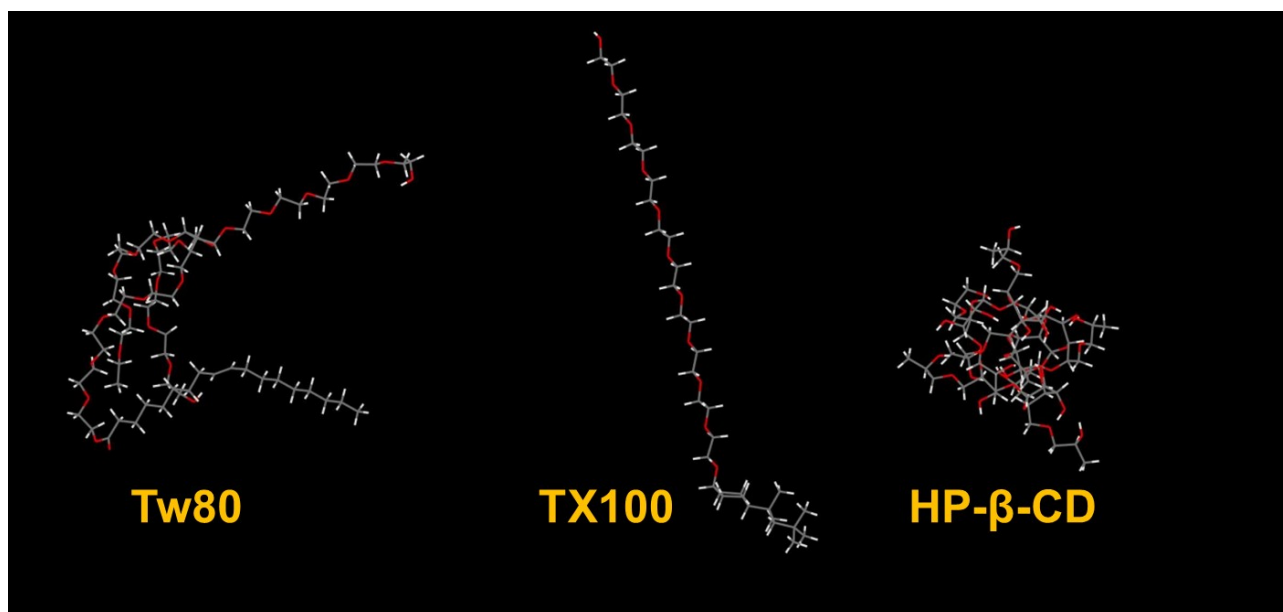


Figure. S10. Numbering of each proton in ^1H NMR of HP- β -CD..



Scheme. 1. The hydrophobic core of HP-β-CD is covered by its HP group. The steric hindrance to the alkyl chain due to the PEG chain is smaller in TX100 than in Tw80. The 3D structures were optimized by PM6 calculations using MOPAC2016. The final heat of formation was -4832 kJ / mol for Tw80, -2166 kJ / mol for TX100, and -7747 kJ / mol for HP-β-CD.